# Influence of Surface Roughness on the Flattening of Powder Particles during Thermal Spraying

### V.V. Sobolev, J.M. Guilemany, and A.J. Martin

The time evolution of the splat thickness, radius, and rate characteristics in the process of flattening of droplets during thermal spraying is investigated taking into account the surface roughness, splat solidification, and mass loss of the droplet liquid phase. Analytical formulas describing the final values of the splat thickness, radius, and rate characteristics are found. Results agree well with the experimental data. They can be used to predict the splat flattening parameters.

## 1. Introduction

KINETICS of flattening of the thermally sprayed molten droplets plays an important role in forming the coating structure and properties (Ref 1). It essentially influences splat size and solidification, adhesion, porosity, inclusions (e.g., oxides), chemical homogeneity, and deposition efficiency.

| Keywords | droplet mass loss, flattening, splat solidification, surface roughness, thermal spraying |
|---|---|

V.V. Sobolev, J.M. Guilemany, and A.J. Martin, Metalurgia Física—Ciencia de Materiales, Departamento de Ingeniería Química y Metalurgia, Universidad de Barcelona, Spain.

Many papers are devoted to the investigation of this problem (Ref 2-8). In the thermal spray processes, the dominant mechanism of the kinetic energy loss is via viscous dissipation. The formulas for the ratio $\xi_f = R_f/R_p$ of the final splat radius, $R_f$, on the initial droplet radius, $R_p$, as a function of the Reynolds number, Re, are given in Ref 4, 6, 7, and 8. Similar formulas for the final splat thickness, $\zeta_f = b_f/R_p$, are given in Ref 8. Analytical expressions describing the time evolution of $\xi$ and $\zeta$ during flattening are also provided in Ref 8.

The developed correlations for $\xi$ and $\zeta$ do not take into account the roughness and nature of the surface on which the particles impact even though experiments show their importance for the correct description and understanding of the droplet flattening (Ref 2).

## Nomenclature

| | | | | |
|---|---|---|---|---|
| $a$ | Reverse impact time, s; $a = U R_p^{-1}$ | | $R_p$ | Particle radius, m |
| $b$ | Splat thickness, m | | Re | Reynolds number; Re $= 2 R_p U \rho/\mu$ |
| $c$ | Sound velocity in a gas-liquid mixture formed during cavitation, ms$^{-1}$ | | $s$ | Sound velocity in a splat liquid phase, ms$^{-1}$ |
| $f$ | Friction coefficient | | $t$ | Time, s |
| $q$ | Specific heat ratio | | $t_s$ | Characteristic time, s; $t_s = \varepsilon/V_s$ |
| $R$ | Splat radius, m | | $U$ | Particle (droplet) impact velocity, ms$^{-1}$ |
| $R_b$ | Gas bubble radius, m | | $V_s$ | Solidification velocity, ms$^{-1}$ |

### Greek Symbols

| | | | | |
|---|---|---|---|---|
| $\alpha$ | Dimensionless roughness parameter; $\alpha = \varepsilon/R_p$ | | $\mu$ | Droplet dynamic viscosity, Nsm$^{-2}$ |
| $\beta$ | $\beta = V_s U^{-1}$ | | $\nu$ | Droplet kinematic viscosity, m$^2$/s |
| $\gamma$ | $\gamma = \exp(0.4\theta)$ | | $\xi$ | Dimensionless splat radius; $\xi = R/R_p$ |
| $\varepsilon$ | Roughness size, m | | $\rho$ | Droplet density, kg/m$^3$ |
| $\zeta$ | Dimensionless splat thickness; $\zeta = b/R_p$ | | $\varphi$ | Gas volume fraction in a gas liquid mixture formed during cavitation |
| $\eta$ | Dimensionless parameter; $\eta = R_p V_s/(\varepsilon U)$ | | | |
| $\theta$ | Dimensionless time; $\theta = at$ | | $\chi$ | Dimensionless parameter of droplet mass loss |
| $\kappa$ | Dimensionless parameter; $\kappa = 0.088 \, \alpha^{1/2}$ | | | |

### Subscripts

| | | | | |
|---|---|---|---|---|
| 0 | Initial | | e | Effective |
| * | Characteristic | | f | Final |
| a | Approximate | | m | Maximum |
| c | Calculated | | s | Solidification |

This paper investigates the influence of the roughness of the substrate surface as well as the roughness of the upper surface of the previously deposited coating layer on the flattening of powder particles during thermal spraying. The splat solidification and mass loss due to splashing and crater formation in the surface where the flattening takes place are considered.

## 2. Main Equations

Assume that a droplet of radius, $R_p$, impinges normally onto the rough surface of a substrate or previously deposited coating layer and forms a cylindrical splat (disk) of radius, $R$, and thickness, $b$, which varies with time during flattening (Fig. 1). Assume further that this rough surface is characterized by the roughness parameter $\alpha_0 = \varepsilon_0/R_p$. After droplet impingement onto the surface, flattening and solidification start. Experiments show that the splat solidification time significantly exceeds that of flattening in the process of thermal spraying (Ref 2). A likely conclusion is that splat solidification is unimportant when flattening is considered. In general, this is not true.

The main heat removal from the splat takes place from its lower part due to the ability of the substrate to transfer heat (Ref 9). This heat removal essentially depends on the substrate and splat thermophysical properties as well as the thermal contact resistance at the splat-substrate (or previously deposited coating layer) interface. It considerably exceeds the heat removal from the splat upper surface (Ref 9).

The solidification front moves from the surface of the substrate or the surface of the already deposited coating layer with a velocity, $V_s$, inside the splat. It gradually decreases the surface roughness and will cover it completely at the time, $t_s = \varepsilon_0 V_s^{-1}$. The degree of splat solidification influence on the part of the flattening process associated with the surface roughness is determined by the ratio, $\eta$, of the impact time $R_p U^{-1}$ to $t_s$, where $U$ is the velocity of the impinging droplet.

$$\eta = \frac{R_p V_s}{\varepsilon_0 U} \qquad \text{(Eq 1)}$$

For example, in the case of plasma spraying of a metallic powder onto an aluminum alloy substrate, when $R_p = 20 \ \mu m$, $V_s = 5 \ ms^{-1}$, $\varepsilon_0 = 1 \ \mu m$, $U = 100 \ ms^{-1}$, from Eq 1, we find that
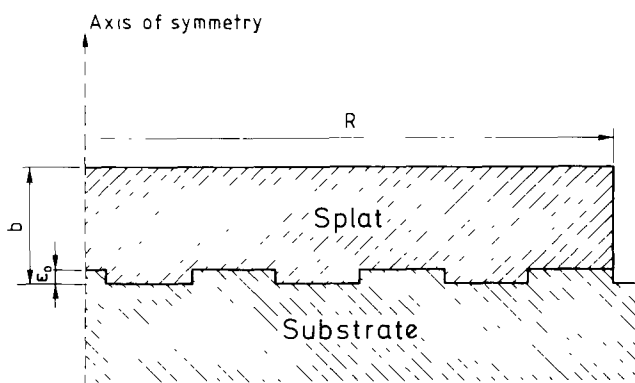


**Fig. 1**   Scheme of a droplet impingement at the substrate surface

$\eta = 1$. Therefore, the solidification must be considered here when the roughness influence on splat flattening is analyzed.

Note that, in this case, the splat solidification influence on flattening must be taken into account even if the surface is smooth. A thin, solidified layer of the splat near the surface, although it is very small, may markedly influence the splat structure and shape (Ref 5, 9).

The increase of the substrate temperature decreases the solidification velocity, $V_s$, and the ratio, $\eta$, and hence, the influence of solidification on the splat flattening. As a result, the splat shapes on smooth substrates may become more regular (Ref 5).

Splat solidification may be slowed down due to the contact thermal resistance between the splat and the underlying surface and to the time delay for nucleation of the solid state because of undercooling of the splat liquid phase when the crystalline structure is formed (Ref 2, 5, 9).

Contact thermal resistance decreases the solidification velocity, $V_s$, which still remains rather high (Ref 2, 9). The ratio $N$ of the nucleation time to the impact time in the case of the homogeneous nucleation was rather high for thermal spray applications (Ref 5). Homogeneous nucleation, though, hardly ever takes place during the thermal spraying due to the presence of inclusions (oxides, carbides, etc.) in the impinging droplet and in the surface microcavities and due to the possible droplet partial solidification before the impingement. Assume that parameter $N$ is markedly smaller than unity and that delays in nucleation do not influence the solidification of the splat lower part during flattening.

To account for the roughness, $\varepsilon$, during the flattening process, assume that it increases the shear stress by the value that arises because of friction between a flattening droplet and the rough surface. Assuming that the flow is turbulent, use the modified Blench formula for the friction coefficient, $f$ (Ref 10). The original equation, $f = 0.79 \ (\varepsilon/D)^{1/2}$, was established for a turbulent flow in a tube of diameter $D$ with a surface roughness $\varepsilon$ provided $\varepsilon << D$. Assume that in the problem of the droplet flattening during thermal spraying, parameter $D$ can be replaced by the initial droplet radius $R_p$ if $\varepsilon << R_p$. Thus:

$$f = 0.79 \ \sqrt{\frac{\varepsilon}{R_p}} = 0.79 \sqrt{\alpha} \qquad \text{(Eq 2)}$$

Also consider that roughness $\varepsilon$ is changed during the splat solidification according to a formula:

$$\varepsilon = \varepsilon_0 - V_s t \qquad \text{(Eq 3)}$$

Qualitatively the same results are obtained when $\varepsilon(t)$ varies with respect to time according to the Stefan "square root" law (Ref 4), which being applied only in the case of solidification of the pure substances, increases the mathematical complexity.

Assume that some part of the mass of an impinging droplet is lost during impact due to splashing and crater formation in the surface where the flattening takes place (Ref 5, 11). This mass loss is determined with the ratio $\chi$ of the droplet mass, which remains after these events to the initial mass of the impinging droplet.

Assume also that the rough surface consists of the rectangular "teeth" with the initial height $\varepsilon_0$. Their length is assumed to

be equal to the distance between them (Fig. 1). Then the variation of the splat thickness, $b$, can be taken as $b - 0.5\,\varepsilon$.

From the mass conservation condition, then:

$$\frac{4}{3} R_p^3 \chi = R^2 (b - 0.5\varepsilon) \qquad \text{(Eq 4)}$$

Reference 4 shows that the splat radius is:

$$R = 2R_p \sqrt{\frac{\chi R_p}{3}} (b - 0.5\varepsilon)^{-1/2} \qquad \text{(Eq 5)}$$

The following equation for splat thickness is obtained using the method and correlations given in Ref 8:

$$b \frac{db}{dt} + 0.4ab^2 + \frac{2}{3} \mu\, \rho^{-1} - \frac{1}{9} U\!f\!b = 0, \qquad a = UR_p^{-1} \qquad \text{(Eq 6)}$$

where $\mu$ and $\rho$ are the dynamic viscosity and density of the molten liquid, respectively.

Introducing the dimensionless variables:

$$\xi = \frac{R}{R_p}, \qquad \zeta = \frac{b}{R_p}, \qquad \alpha = \frac{\varepsilon}{R_p}, \qquad \beta = \frac{V_s}{U}, \qquad \theta = at \qquad \text{(Eq 7)}$$

from Eq 5 and 6, the following equations are obtained:

$$\xi = 2\sqrt{\frac{\chi}{3}} (\zeta - 0.5\alpha)^{-1/2} \qquad \text{(Eq 8)}$$

$$\zeta \frac{d\zeta}{d\theta} + 0.4\zeta^2 + \frac{4}{3\mathrm{Re}} - \kappa\zeta = 0 \qquad \text{(Eq 9)}$$

and

$$\mathrm{Re} = \frac{2R_p U\rho}{\mu}, \qquad \kappa = 0.088\sqrt{\alpha}, \qquad \alpha = \alpha_0 - \beta\theta$$

## 3. Results and Discussion

### 3.1 *Analytical Formulas*

Assuming that surface roughness is small ($\kappa \ll 1$) and representing the solution of Eq 9 in a form of series with respect to $\kappa$, the following expression is obtained for the splat thickness, $\zeta$, when $\mathrm{Re} \gg 1$ with an accuracy of the order of $0\,(\kappa^2)$:

$$\zeta = \gamma^{-1}[1 + 0.22\sqrt{\alpha}(\gamma - 1)], \qquad \gamma = \exp(0.4\theta) \qquad \text{(Eq 10)}$$

Substituting Eq 10 in Eq 8, then, with the same accuracy:

$$\xi = 2\sqrt{\frac{\chi\gamma}{3}} [1 - 0.11\sqrt{\alpha}(\gamma - 1)] \qquad \text{(Eq 11)}$$

From Eq 10 and 11, the rate characteristics of the flattening process are also obtained:

$$\frac{d\zeta}{d\theta} = -0.4\gamma^{-1} [1 - 0.22\sqrt{\alpha} + 0.275\,\eta\,\sqrt{\alpha}(\gamma - 1)] \qquad \text{(Eq 12)}$$

$$\frac{d\xi}{d\theta} = 0.4\sqrt{\frac{\chi\gamma}{3}} [1 - 0.11\sqrt{\alpha}(3\gamma - 1) + 0.275\,\eta\sqrt{\alpha}(\gamma - 1)] \qquad \text{(Eq 13)}$$

For the smooth surface ($\alpha = 0$) and without the mass loss ($\chi = 1$) from Eq 10 to 13, we have the formulas obtained in Ref 8. From the analytical expressions (Eq 10-13), it follows that the increase of the surface roughness increases the flattening splat thickness and decreases the splat radius and the rate characteristics of the flattening process $|db/dt|$ and $dR/dt$. The last terms on the right-hand sides of Eq 12 and 13 reflect the influence of splat solidification, which decreases surface roughness and, therefore, contributes to the increase of $dR/dt$ and $|db/dt|$.

Reference 8 shows that the analytical results obtained are valid up to $t \le t_*$ within the framework of the approximation used to derive them. Parameter $t_*$ is defined by the formula:

$$t_* = \frac{5R_p}{6U} \ln (1 + 0\,3\mathrm{Re}) \qquad \text{(Eq 14)}$$

Reference 8 shows that the values of $b$ and $R$ at $t = t_*$ correspond approximately to the final values $b_f$ and $R_f$ of the splat thickness $b$ and radius $R$ when the droplet flattens onto the smooth surface ($\varepsilon = 0$). Assume that the same is likely to occur when the droplet flattening takes place on the rough surface ($\varepsilon \ne 0$) and that in this case the values of the flattening parameters at $t = t_*$ may also be considered as their approximate final values. The value of $t_*$ corresponds to the following value of $\theta_*$:

$$\theta_* = \frac{5}{6} \ln (1 + 0.3\mathrm{Re}) \qquad \text{(Eq 15)}$$

Substituting $\theta = \theta_*$ in Eq 10 to 13 gives:

$$\zeta_f = 1.83\,\mathrm{Re}^{-1/2} (1 + 0.22\,y\sqrt{\alpha}) \qquad \text{(Eq 16)}$$

$$\xi_f = 0.8546\sqrt{\chi}\,\mathrm{Re}^{1/4} (1 - 0.11\,y\sqrt{\alpha}) \qquad \text{(Eq 17)}$$

$$\frac{d\zeta_f}{d\theta} = -0.73\,\mathrm{Re}^{-1/2} (1 - 0.22\sqrt{\alpha} + 0.275\,y\eta\sqrt{\alpha}) \qquad \text{(Eq 18)}$$

$$\frac{d\xi_f}{d\theta} =$$

$$0.17\sqrt{\chi}\,\mathrm{Re}^{1/4} [1 - 0\,11\sqrt{\alpha}(1.643\,\mathrm{Re}^{1/2} - 1) + 0.275\,y\eta\sqrt{\alpha}]$$

$$y = 0.548\,\mathrm{Re}^{1/2} - 1 \qquad \text{(Eq 19)}$$

When $\mathrm{Re} \gg 1$, Eq 16 to 19 give:

$$\zeta_f = 1.83\,\mathrm{Re}^{-1/2} (1 + 0.12\sqrt{\alpha}\,\mathrm{Re}^{1/2}) \qquad \text{(Eq 20)}$$

$$\xi_f = 0.8546 \sqrt{\chi} \ Re^{1/4} (1 - 0.06 \sqrt{\alpha} Re^{1/2}) \qquad \text{(Eq 21)}$$

$$\frac{d\zeta_f}{d\theta} = -0.73 \ Re^{-1/2} (1 - 0.22 \sqrt{\alpha} + 0.15 \eta \sqrt{\alpha} Re^{1/2}) \qquad \text{(Eq 22)}$$

$$\frac{d\xi_f}{d\theta} = 0.17 \sqrt{\chi} \ Re^{1/4} [1 - 0.18 \sqrt{\alpha}(1 - 0.83 \eta) Re^{1/2}] \qquad \text{(Eq 23)}$$

For the smooth surface ($\alpha = 0$) and without the mass loss ($\chi = 1$) from Eq 20 to 23, we have the formulas obtained in Ref 8. From Eq 20 to 23, it follows that increase of the surface roughness increases the splat final thickness, decreases its final radius, and decreases the variation rate of $\xi$ and the absolute value of the variation rate of $\zeta$. The formula (Eq 20) shows that under the

high Reynolds numbers (Re >> 1), the influence of surface roughness on the splat final thickness does not depend on Re.

From the above analysis, it follows that the influence of the surface roughness is equivalent to the influence of an effective viscosity $\mu_e$. Use of the analytical expressions (Eq 20, 21) shows that this effective viscosity with an accuracy of the order of $0(\alpha)$ is as follows:

$$\mu_e = \mu(1 + 0.24 \sqrt{\alpha} \ Re^{1/2}) \qquad \text{(Eq 24)}$$

Then Eq 20 and 21 can be written as:

$$\zeta_f = 1.83 \ Re_e^{-1/2} \qquad \text{(Eq 25)}$$

$$\xi_f = 0.8546 \sqrt{\chi} \ Re_e^{1/4}, \qquad Re_e = \frac{2R_p U \rho}{\mu_e} \qquad \text{(Eq 26)}$$

Note that the splat solidification may also contribute to the increase of the splat liquid phase viscosity because the rheological properties of the solidifying substance become pronounced at the temperatures in the thermal interval of solidification (for alloys) or near solidification point (for pure substances) (Ref 12, 13).

When cavitation takes place during coating deposition, a gas-liquid mixture is formed (Ref 14, 15). This mixture viscosity markedly exceeds the pure liquid viscosity due to the energy dissipation on the gas bubbles (Ref 16, 17). The effective kinematic viscosity, $v_e$, in this case, is (Ref 17):

$$v_e = \frac{\mu}{3\varphi\rho} + \frac{R_b c^2 q}{s} \qquad \text{(Eq 27)}$$

where $\varphi$ is the gas volume fraction; $R_b$ is the gas bubble radius; $c$ and $s$ are the sound velocities in the gas-liquid mixture and the splat liquid phase, respectively; and $q$ is the specific heat ratio.

The first term on the right-hand side of Eq 27 represents the viscous dissipation; the second term there describes the dissipation due to acoustic radiation.
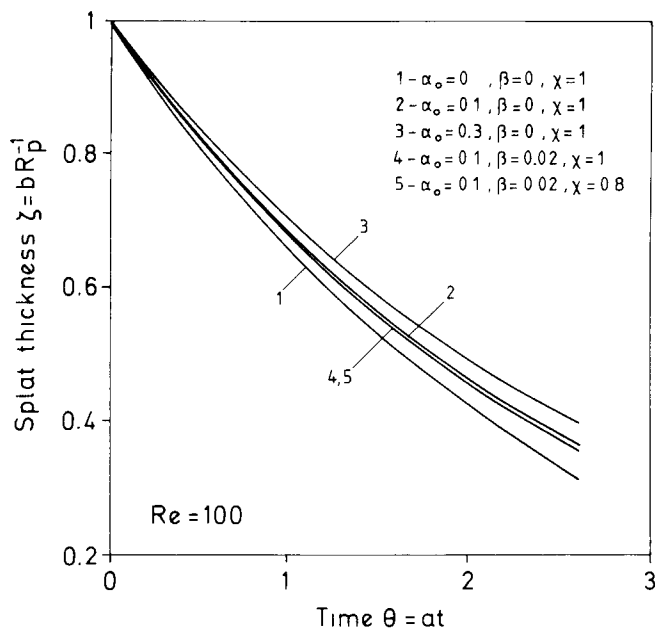
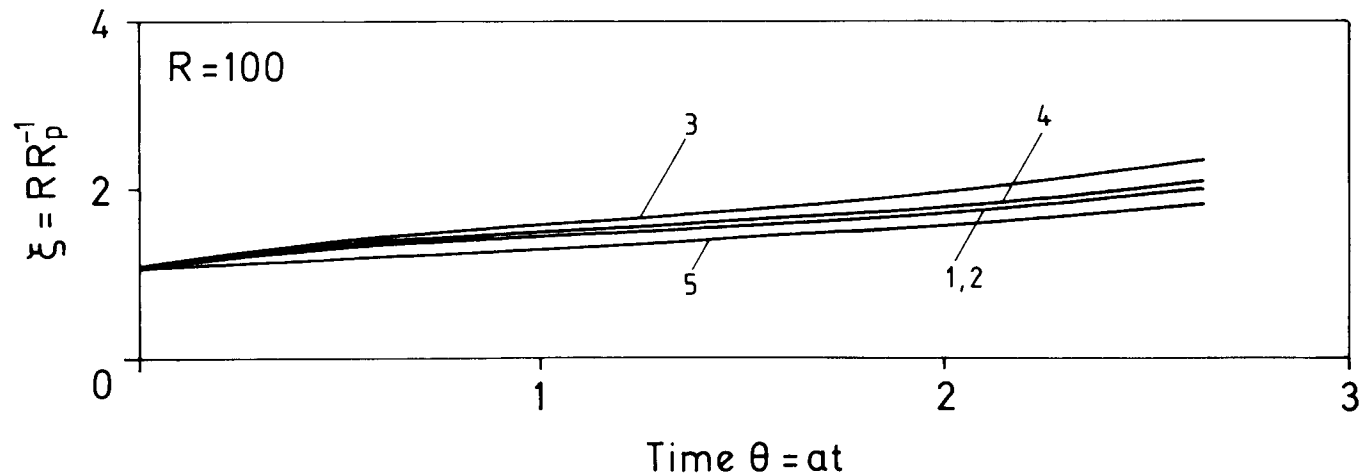

Fig. 2  Variation of the splat thickness with time



Fig. 3  Variation of the splat radius with time. Curve numbers correspond to the parameters shown in Fig. 2.

The mentioned phenomena contribute to the increase of the viscosity of the splat liquid phase; hence, they increase the flattening splat thickness and decrease its radius.

The splat final radius varies nonuniformly with respect to the Reynolds number and, as follows from Eq 21 or 26, achieves the maximum value $\xi_m$ at $Re = Re_m$.

$$Re_m = 30.86\,\alpha^{-1} \tag{Eq 28}$$

$$\xi_m = 1.34\,\sqrt{\chi}\,\alpha^{-1/4} \tag{Eq 29}$$

Both $Re_m$ and $\xi_m$ decrease with the increase of the roughness parameter $\alpha$; $\xi_m$ decreases more slowly than $Re_m$.

Use of Eq 19 shows that the rate of the splat radius variation $d\xi/d\theta$ is also a nonuniform function of the Reynolds number and attains the maximum value when $Re = Re_m$. Here:

$$Re_m \approx \alpha^{-1} \tag{Eq 30}$$

The basic assumption used to obtain the above results on the transient and final characteristics of flattening is that most of the kinetic energy of the impinging droplet is dissipated due to viscous effects (Ref 4, 8). This agrees with the experimental data (Ref 3-7). Meanwhile a small part of the kinetic energy of the impinging droplet is transformed in the surface energy. This occurs mostly at the final stage of the flattening process when surface tension effects start to dominate over those of inertia due to the flattening velocity decrease (Ref 4-6).

Flattening parameters given by Eq 16 to 23 correspond to the time required to reach about 90% completion of flattening. This limit represents a convenient parameter to determine the flattening characteristics (Eq 16-23) due to the inherent asymptotic behavior of the flattening process (Ref 6).

### 3.2 Numerical Simulation

To study the transient characteristics of the flattening process, Eq 9 for the splat thickness, $\zeta$, was solved numerically by the method of Runge-Kutta with an initial condition:

$$\zeta(0) = 1 \tag{Eq 31}$$

Then, from the formula (Eq 8), the splat radius, $\xi$, was found.

Figure 2 shows that the splat thickness increases with the increase of the roughness parameter $\alpha_0$. Under the same value of $\alpha_0$, the splat thickness decreases when the solidification occurs in the lower part of the splat, which diminishes the roughness. The splat thickness variation is not sensitive to the mass loss of an impinging droplet.

The decrease of the splat thickness, $\zeta$, leads to the increase of the splat radius, $\xi$ (Fig. 3). When the roughness increases, there are two competitive tendencies in the behavior of the splat radius. (See Eq 8.) The increase of $\alpha$ causes the increase of $\zeta$ and hence the decrease of splat radius $\xi$. At the same time, the increase of roughness, according to Eq 4 and 8, provokes the increase of the splat radius.

When the first tendency takes place, i.e., when the increase of the roughness influences the splat radius mainly through the increase of the splat thickness, the value of $\xi$ diminishes with the increase of $\alpha$. When the second tendency takes place, the in-

**Table 1  Comparison of numerical and analytical values of $Re_m$ and $\xi_m$**

| $\alpha_0$ | $\eta$ | $\chi$ | $Re_m^{(c)}$ | $Re_m^{(a)}$ | $\omega_1$ | $\xi_m^{(c)}$ | $\xi_m^{(a)}$ | $\omega_2$ |
|---|---|---|---|---|---|---|---|---|
| 0.03 | 0 | 1 | 1060 | 1029 | 2.9 | 3.312 | 3.220 | 2.8 |
| 0.03 | 0.5 | 0 8 | 1060 | 1029 | 2 9 | 2.963 | 2 880 | 2.8 |
| 0.1 | 0 | 1 | 328 | 309 | 5 8 | 2.508 | 2.383 | 5.0 |
| 0.5 | 0 | 1 | 71 | 62 | 12.7 | 1 783 | 1.594 | 10 6 |

$\omega_1$ (%) $\equiv [Re_m^{(c)} - Re_m^{(a)}]/Re_m^{(c)}$; $\omega_2$ (%) = $[\xi_m^{(c)} - \xi_m^{(a)}]/\xi_m^{(c)}$
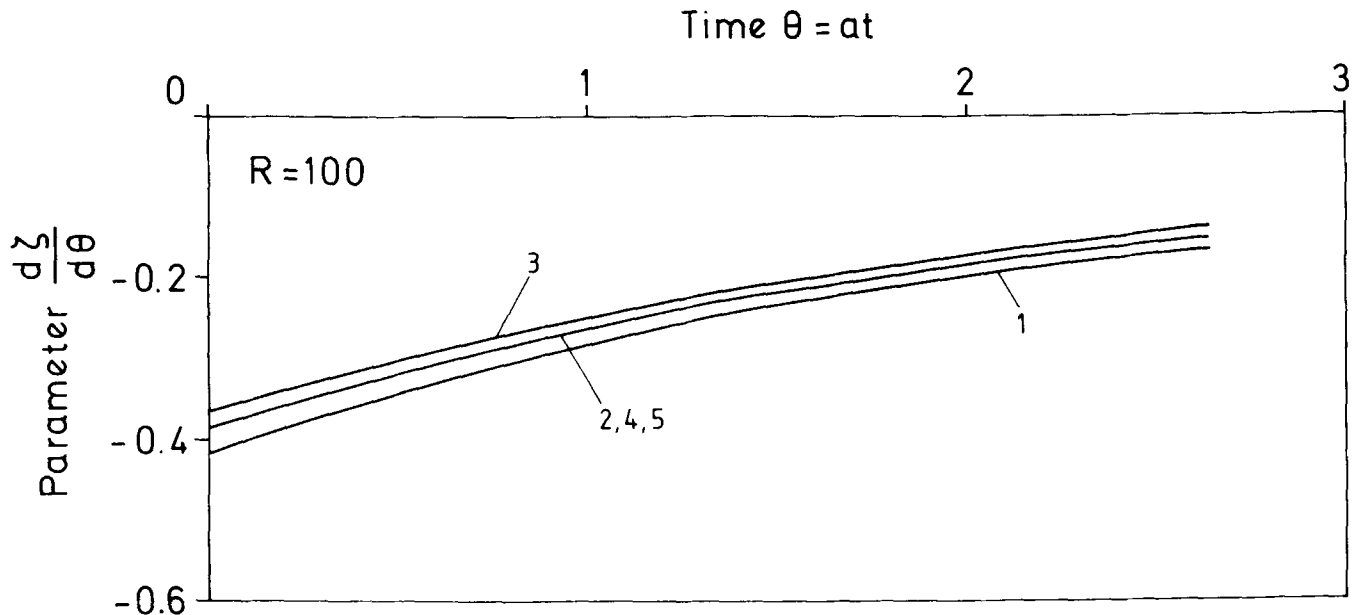


**Fig. 4** Dependence of rate of splat thickness variation on time  Curve numbers correspond to the parameters shown in Fig 2

crease of roughness causes the increase of splat radius (curve 3 in Fig. 3). Solidification decreases surface roughness and thus contributes to the increase of $\xi$ (curve 4 in Fig. 3). The mass losses lead to the decrease of splat radius.

Figure 4 shows that the absolute value of the variation rate of the splat thickness $d\zeta/d\theta$ decreases with time. When the roughness increases, the absolute value of $d\zeta/d\theta$ diminishes. When the splat solidification occurs, the parameter $|d\zeta/d\theta|$ generally increases. Here this increase is very small.

For the practice of thermal spraying, it is important also to know the variations of the final values of $\zeta$ and $\xi$ as well as the rate parameters of flattening, which are determined with Eq 16 to 19 and 20 to 23. The not very high values of Re were considered by studying the analytical expressions, Eq 16 to 19.
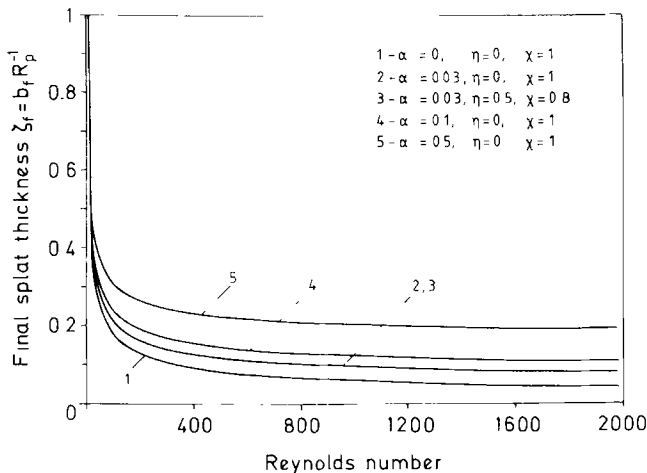


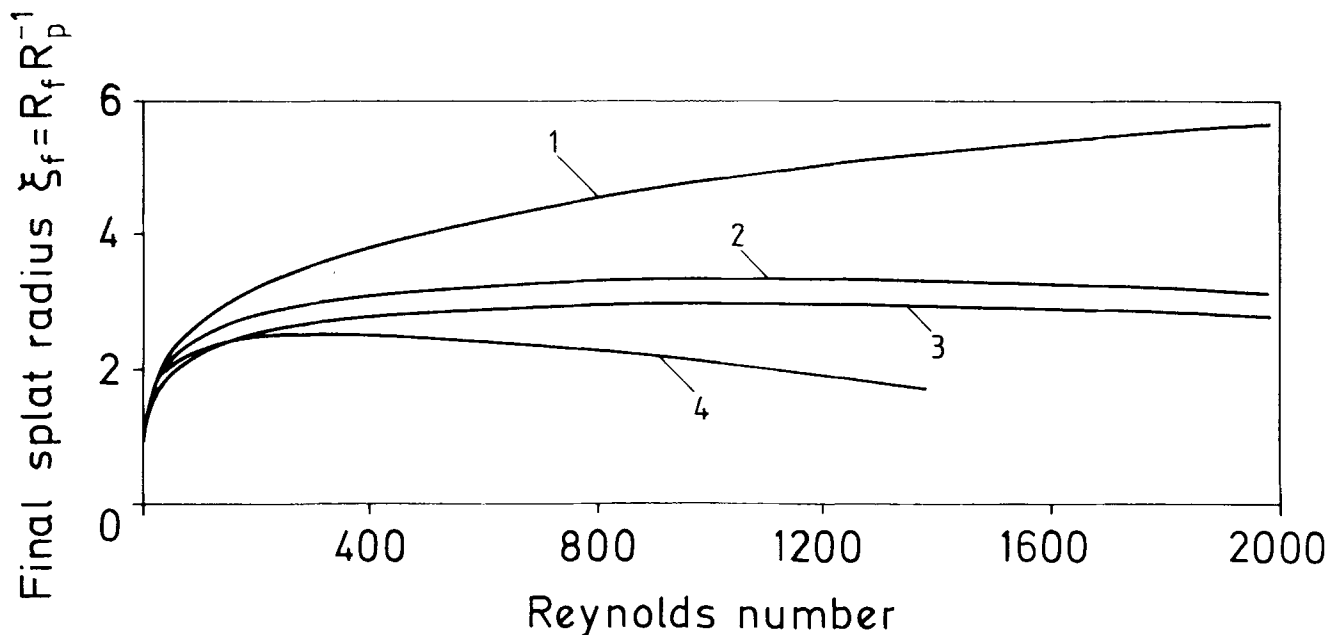**Fig. 5** Variation of the final splat thickness with the Reynolds number

The final value of the splat thickness, $\zeta_f$, decreases with the Reynolds number and increases with the surface roughness (Fig. 5). The parameter $\eta$ has practically no influence on $\zeta_f$.

Figure 6 shows that the final splat radius increases with Re when the surface is smooth (curve 1 with $\alpha = 0$) and exhibits the nonuniform behavior with respect to the Reynolds number when the flattening takes place at a rough surface. In this case, the value of $\xi_f$ first increases, attains the maximum value, and then decreases.

Table 1 compares the numerical (calculated) values $\xi_m^{(c)}$ and $Re_m^{(c)}$, respectively, of the maximum $\xi_m$ of the splat radius $\xi$ and the Reynolds number $Re = Re_m$ corresponding to it with their approximate values $\xi_m^{(a)}$ and $Re_m^{(a)}$, respectively. The $\xi_m^{(c)}$ and $Re_m^{(c)}$ were determined from the numerical tabulation of Eq 17, whereas $\xi_m^{(a)}$ and $Re_m^{(a)}$ were found from Eq 28 and 29. The maximum value $\xi_m$ decreases with the surface roughness increase and mass loss. The Reynolds number $Re_m$ corresponding to $\xi_m$ also diminishes when the surface roughness increases.

The differences between $\xi_m^{(c)}$ and $\xi_m^{(a)}$ as well as between $Re_m^{(c)}$ and $Re_m^{(a)}$ are small and increase with $\alpha_0$. This means that for practical purposes, the parameters $R_m$ and $\xi_m$ can be determined from Eq 28 and 29, respectively, which correspond to $Re \gg 1$.

The absolute value of the final rate of the splat thickness variation $d\zeta/d\theta$ decreases with the Reynolds number, and the velocity of this decrease diminishes with Re (Fig. 7). The surface roughness decreases the absolute value of $d\zeta/d\theta$, whereas the splat solidification contributes to its increase.

Figure 8 shows that the final rate of the splat radius variation $d\xi/d\theta$ increases with the Reynolds number in the case of the smooth surface ($\alpha = 0$). Its behavior becomes nonuniform with respect to Re when the flattening takes place at a rough surface. In this case, the parameter $d\xi/d\theta$ first increases, achieves the maximum value, and then decreases.



**Fig. 6** Variation of the final splat radius with the Reynolds number. Curve numbers correspond to the parameters shown in Fig. 5.

The position of the maximum $Re_m$ is well determined with Eq 30. The roughness increase causes the decrease of $d\xi/d\theta$, which becomes negative when $\alpha$ is rather high. Splat solidification leads to the increase of $d\xi/d\theta$.

Remember that although the values of $d\zeta_f/d\theta$ and $d\xi_f/d\theta$ in Fig. 7 and 8 are small (with an exception of curve 5 in Fig. 8, which is given for illustrative purposes), they are not equal to zero as expected at the termination of the flattening process. This is because of the approximate nature of Eq 18 and 19, as discussed.

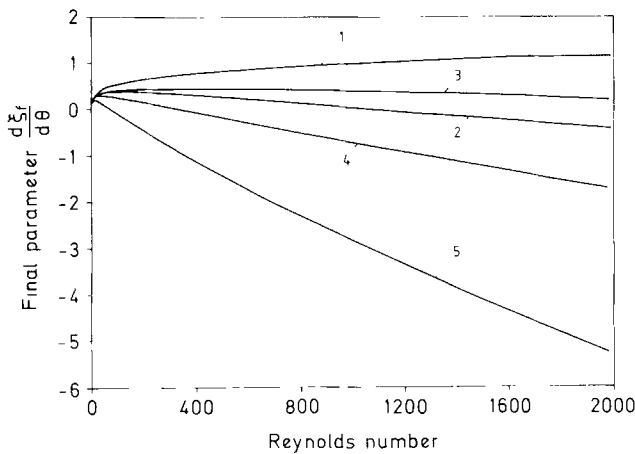### 3.3 Comparison with Experimental Data

Reference 8 showed that the equations obtained for the final values of the splat radius and thickness agree well with the experimental data when the droplet flattening took place at a smooth surface ($\alpha = 0$). Reference 8 also demonstrated that a parameter that followed from Eq 14 and described a characteristic flattening time agreed with a similar parameter introduced in Ref 6 for the practical purposes of thermal spraying.

Figure 9 compares the final splat radius $\xi_f$ calculated with Eq 17 with the experimental data for the zirconia particles impacting on a steel substrate at 75 °C in the process of plasma spraying (Ref 3).

As the substrate is relatively "cold," the splashing should be more pronounced. Splat solidification should have more influence on the flattening process (Ref 3, 5), which means the final substrate surface roughness is not high.

The theoretical curves in Fig. 9 show that when the surface roughness and the droplet mass loss are taken into account, the theoretical results fit the experimental data better than those that do not account for those factors (Ref 4).

The experimental results obtained in Ref 3 were rather consistent with the values of the final splat radius given in Ref 7. The difference between the equations of Madejski (Ref 4) and Yosida (Ref 7) is that Yosida gives about 36% smaller values of $\xi$ than Madejski. The Yosida equation gives results that are qualitatively the same as the equations for $\xi$ that take into account the surface roughness and the droplet mass loss. That is

why the Yosida equation agrees with the experimental results of Ref 3.

Thus, the results obtained agree well with the observed tendencies of the splat flattening and with the experimental data.

## 4. Conclusions

The approximate equations describing the time evolution of the thermally sprayed splat thickness and radius as well as their variation rates during the flattening process are established taking into account the surface roughness of the droplet impingement, the splat solidification, and the loss of the droplet mass due to splashing and crater formation in the surface.

The realistic correlations between the final values of the splat thickness, splat radius, and their variation rates, and the Reynolds number are obtained by taking into account the mentioned phenomena.

An effective dynamic viscosity of the splat liquid phase is introduced that accounts for the surface roughness influence on the droplet flattening during thermal spraying.
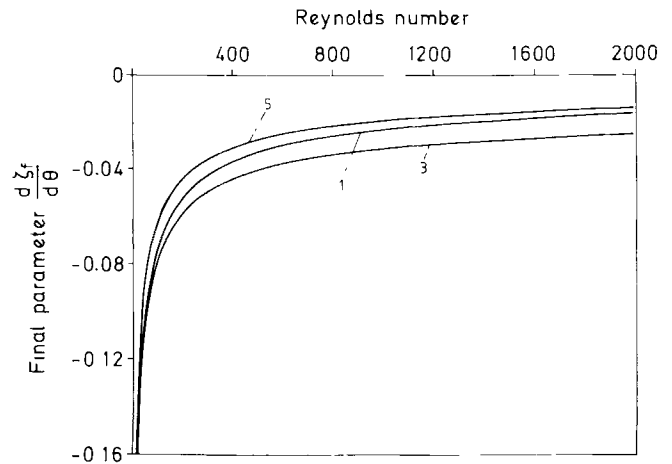


**Fig. 7** Dependence of final rate of splat thickness variation on the Reynolds number. Curve numbers correspond to the parameters shown in Fig. 5



**Fig. 8** Dependence of final rate of splat radius variation on the Reynolds number Curve numbers correspond to the parameters shown in Fig 5.
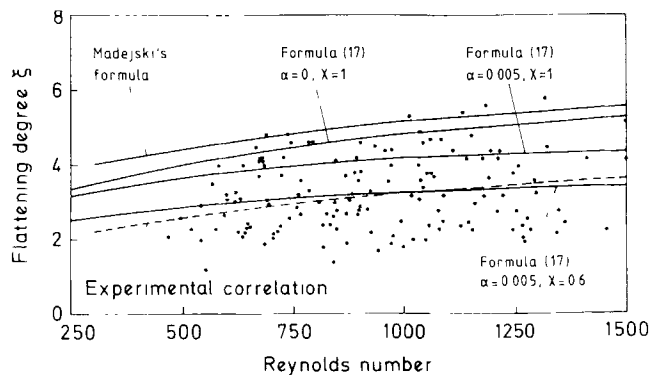


**Fig. 9** Comparison of analytical and experimental results describing final splat radius (flattening degree). Data points indicate experimental results from Ref 3.

Splat thickness increases with the roughness increase and decreases when solidification takes place in the lower part of the splat. The splat thickness variation is not sensitive to the mass loss of the impinging droplet.

When the surface roughness increases, there are two competitive tendencies in the time evolution of the splat radius. On the one hand, the roughness increase causes the increase of the splat thickness and, hence, the decrease of the splat radius. On the other hand, the roughness directly influences the splat radius causing its increase. As a result, splat radius either diminishes or increases with surface roughness. Solidification decreases surface roughness and contributes to the increase of splat radius. Droplet mass loss leads to the decrease of splat radius.

The absolute value of the splat thickness rate variation decreases with time. When the roughness increases, the absolute value of the variation rate of the splat thickness diminishes. Under the splat solidification, this absolute value increases.

The final value of the splat thickness decreases with Reynolds number and increases with surface roughness. The final splat radius increases with the Reynolds number when the surface is smooth and exhibits nonuniform behavior with respect to Reynolds number in the case of rough surface. In this case, the final splat radius first increases, attains the maximum value, and then decreases. The analytical expressions are obtained for the maximum value of the final splat radius and the Reynolds number that corresponds to it.

The absolute value of the final rate of the splat thickness variation decreases with the Reynolds number. The surface roughness diminishes this absolute value whereas the splat solidification increases it. The final rate of the splat radius variation increases with the Reynolds number when the surface is smooth and demonstrates nonuniform behavior with respect to the Reynolds number when the surface is rough. In this case, the final rate of the splat radius variation first increases, achieves the maximum value, and then diminishes. The surface roughness increase causes the decrease of this parameter, and the splat solidification leads to its increase.

Theoretical results obtained for the final splat radius agree well with the experimental data. Analytical expressions for the final parameters of the flattening process can be used for prediction purposes.

## Acknowledgments

## References

1  R. McPherson, The Relationship between the Mechanism of Formation, Microstructure and Properties of Plasma Sprayed Coatings, *Thin Solid Films*, Vol 83, 1981, p 297-310

2  C. Moreau, P Cielo, and M. Lamontagne, Flattening and Solidification of Thermally Sprayed Particles, *J. Therm. Spray Technol.*, Vol 1, 1992, p 317-323

3. S. Fantassi, M. Vardelle, A. Vardelle, and P. Fauchais, Influence of the Velocity of Plasma Sprayed Particles on Splat Formation, *J. Therm. Spray Technol.*, Vol 2 (No. 4), 1993, p 379-384

4  J Madejski, Solidification of Droplets on a Cold Surface, *Int. J. Heat Mass Transfer*, Vol 19, 1976, p 1009-1013

5. R.C. Dykhuizen, Review of Impact and Solidification of Molten Thermal Spray Droplets, *J. Therm. Spray Technol.*, Vol 3 (No. 4), 1994, p 351-361

6. G. Trapaga and J Szekely, Mathematical Modelling of the Isothermal Impingement of Liquid Droplets in Spraying Processes, *Metall. Trans. B*, Vol 22, 1991, p 901-914

7  T.Y. Yosida, T. Okada, H. Hamatani, and H. Kumaoka, Integrated Fabrication Process for Solid Oxide Fuel Cells Using Novel Plasma Spraying, *Plasma Sources Sci. Technol.*, Vol 1, 1992, p 195-201

8. V.V Sobolev and J.M. Guilemany, Flattening of Thermally Sprayed Particles, *Mater. Lett.*, Vol 22, 1995, p 209-213

9  V.V. Sobolev, J.M. Guilemany, and J.A. Calero, Substrate-Coating Thermal Interaction during High Velocity Oxy-Fuel (HVOF) Spraying. Part 1. Heat Transfer Processes, *Mater. Sci. Technol.*, Vol 11 (No. 8), 1995, p 810-819

10. R. Ouziaux and J. Perrier, *Mécanique des Fluides Appliquée. Tome 1. Fluides Incompressibles*, Dunad, Paris, 1972, p 217-221

11. R. Tiwari and H Herman, Incorporation of Reinforcements in Spray Formed MMCs, *Scr. Metall. Mater.*, Vol 25, 1991, p 1103-1107

12. V.V. Sobolev and P.M. Trefilov, *Particular Features of Dynamic Processes in Mushy Zone of Solidifying Melt*, Comm Acad. Sci USSR Metals, No. 5, 1983, p 72-77 (in Russian)

13  V.V. Sobolev, On Propagation of Disturbances in Viscoelastic Gas-Liquid Medium, *Nonlinear Wave Processes in Gas-Liquid Media*, Inst. Thermophysics, Sib. Br Acad. Sci. USSR, Novosibirsk, 1977, p 45-53 (in Russian)

14. Y.C. Huang, F G. Hammit, and W.-J Yang, Hydrodynamic Phenomena during High-Speed Collision between Liquid Droplet and Rigid Plane, *Trans. ASME, J. Fluids Eng.*, June 1973, p 276-294

15. O G. Engel, Waterdrop Collisions with Solid Surfaces, *J. Res. Natl. Bur. Stand.*, Vol 54 (No. 5), 1995, p 281-298

16. V.V Sobolev and P.M. Trefilov, *Thermophysics of Metal Solidification during Continuous Casting*, Metallurgy, Moscow, 1988 (in Russian)

17. V V Sobolev and P M. Trefilov, *Heat and Mass Transfer Processes during Solidification of Continuous Ingots*, Krasnoyarsk University Press, Krasnoyarsk, 1984 (in Russian)